LOCKHEED MARTIN ENERGY RESEARCH LIBRARIES

H LIBRARY

3 4456 0514776 6

ORNL-TM-3864

cy. 38

EFFECTS OF AIR-DENSITY PERTURBATIONS ON THE TRANSPORT OF NEUTRONS AND SECONDARY GAMMA RAYS PRODUCED BY POINT NEUTRON SOURCES

B. J. McGregor

Lorraine S. Abbott

OAK RIDGE NATIONAL LABORATORY
CENTRAL RESEARCH LIBRARY
DOCUMENT COLLECTION

LIBRARY LOAN COPY

DO NOT TRANSFER TO ANOTHER PERSON

If you wish someone else to see this document, send in name with document and the library will arrange a loan.

UCN-7969
(3 3-67)

OAK RIDGE NATIONAL LABORATORY

OPERATED BY UNION CARBIDE CORPORATION • FOR THE U.S. ATOMIC ENERGY COMMISSION

This report was prepared as an account of work sponsored by the United States Government. Neither the United States nor the United States Atomic Energy Commission, nor any of their employees, nor any of their contractors, subcontractors, or their employees, makes any warranty, express or implied, or assumes any legal liability or responsibility for the accuracy, completeness or usefulness of any information, apparatus, product or process disclosed, or represents that its use would not infringe privately owned rights.

ORNL-TM-3864

Contract No. W-7405-eng-26

Neutron Physics Division

EFFECTS OF AIR-DENSITY PERTURBATIONS ON THE TRANSPORT OF NEUTRONS AND SECONDARY GAMMA RAYS PRODUCED BY POINT NEUTRON SOURCES

Work Done by:

B. J. McGregor*

Report Written by:

B. J. McGregor*
Lorraine S. Abbott

AUGUST 1972

NOTE:

This Work Funded by
DEFENSE NUCLEAR AGENCY
Under Subtask PC050-03

*On assignment from the Australian Atomic Energy Commission.

OAK RIDGE NATIONAL LABORATORY
Oak Ridge, Tennessee 37830
operated by
Union Carbide Corporation
for the
U.S. ATOMIC ENERGY COMMISSION

LOCKHEED MARTIN ENERGY RESEARCH LIBRARIES

3 4456 0514776 6

Abstract

A series of MORSE Monte Carlo calculations have been performed to determine the effect that changes in the air density produced by one weapon detonation would have on the transport of radiation produced by a second weapon detonated within the next few seconds. The responses of interest were the displacement and ionization that would be induced in silicon by neutrons and secondary gamma rays respectively in the vicinity of the first burst. Two density profiles around the first burst were used, corresponding to times of 1 and 3.16 sec after the burst. Three neutron emission spectra were used for the second weapon, one consisting of 14-MeV neutrons alone and the other two consisting of typical thermonuclear and ^{235}U fission spectra. In all cases the medium was assumed to be infinite air, and spherical geometry was employed with the origin at the center of the first detonation. The responses were calculated for eight distances from the second source in the direction of the first source within seven (or nine) solid angles measured from an axis passing through both sources. For the 3.16-sec density profile and source separation distances of 1100 and 1500 m the density perturbation effects at the points of interest were small. The effects were much more pronounced for the 1-sec profile, which is partially due to the two sources being closer together (0 to 800 m). With the 1-sec profile all neutron responses calculated for positions immediately beyond the first burst were about 50% higher than those obtained at the same positions in the unperturbed atmosphere; lesser increases were obtained as the angle from the axis of symmetry was increased. The secondary gamma-ray responses also were higher, with the increases being approximately one-half of the increase in the neutron responses for the same positions. For the case of the two detonations occurring at the same position, the neutron responses between 1000 and 1500 m were about 20% higher than those in the unperturbed atmosphere and the gamma-ray responses were 10% higher.

Table of Contents

		Page No.
	Abstract	iii
I.	Introduction	1
II.	Calculational Procedure	1
III.	Displacement and Ionization Responses for Unperturbed Atmosphere	8
IV.	Displacement and Ionization Responses for Perturbed Atmosphere	13
V.	Neutron and Gamma-Ray Fluxes Produced by 14-MeV Neutron Source	17
VI.	Importance of 14-MeV Neutrons Born at Radius R to Responses at Origin of Spherical Geometry	20
VII.	Summary	20

EFFECTS OF AIR-DENSITY PERTURBATIONS ON THE TRANSPORT OF NEUTRONS AND SECONDARY GAMMA RAYS PRODUCED BY POINT NEUTRON SOURCES

B. J. McGregor

I. Introduction

Several calculations have been performed to investigate the effect that changes in the air density produced by one weapon detonation would have on the transport of radiation produced by a second weapon detonated within the next few seconds. The density of the unperturbed air was taken to be 4.5×10^{-4} g/cc, which is the density that would exist at an altitude of about 9.15 km. In all cases the density profile of the perturbed air was assumed to be spherically symmetric around the point of detonation of the first weapon, and the second weapon was assumed to be a point isotropic neutron source emitting neutrons of specified energies at given distances from the first source. The radiations considered were the neutrons emitted from the second source and the secondary gamma rays produced by interactions of those neutrons in the atmosphere. The results are given in terms of the neutron displacement and gamma-ray ionization in silicon.

II. Calculational Procedure

Two density profiles around the first weapon were used, one describing the air density as a function of distance from the weapon at a time 3.16 sec after the burst (see Fig. 1), and another giving the same information at a time 1 sec after the burst (see Fig. 2). Three different emission spectra were used for the second source; a spectrum typical of a thermonuclear weapon[1] (see Table 1); a spectrum consisting of 14-MeV neutrons alone; and a spectrum typical of ^{235}U fission neutrons.

The cases for which the calculations were performed are shown in Table 2. In all calculations the medium was assumed to be infinite air, and spherical geometry was used with the origin at the center of the first detonation (see Figs. 3-8). Neutron and gamma-ray responses were calculated for eight distances from the second source within seven (or nine) solid angles. The distances are defined as the midpoints of radial bins as

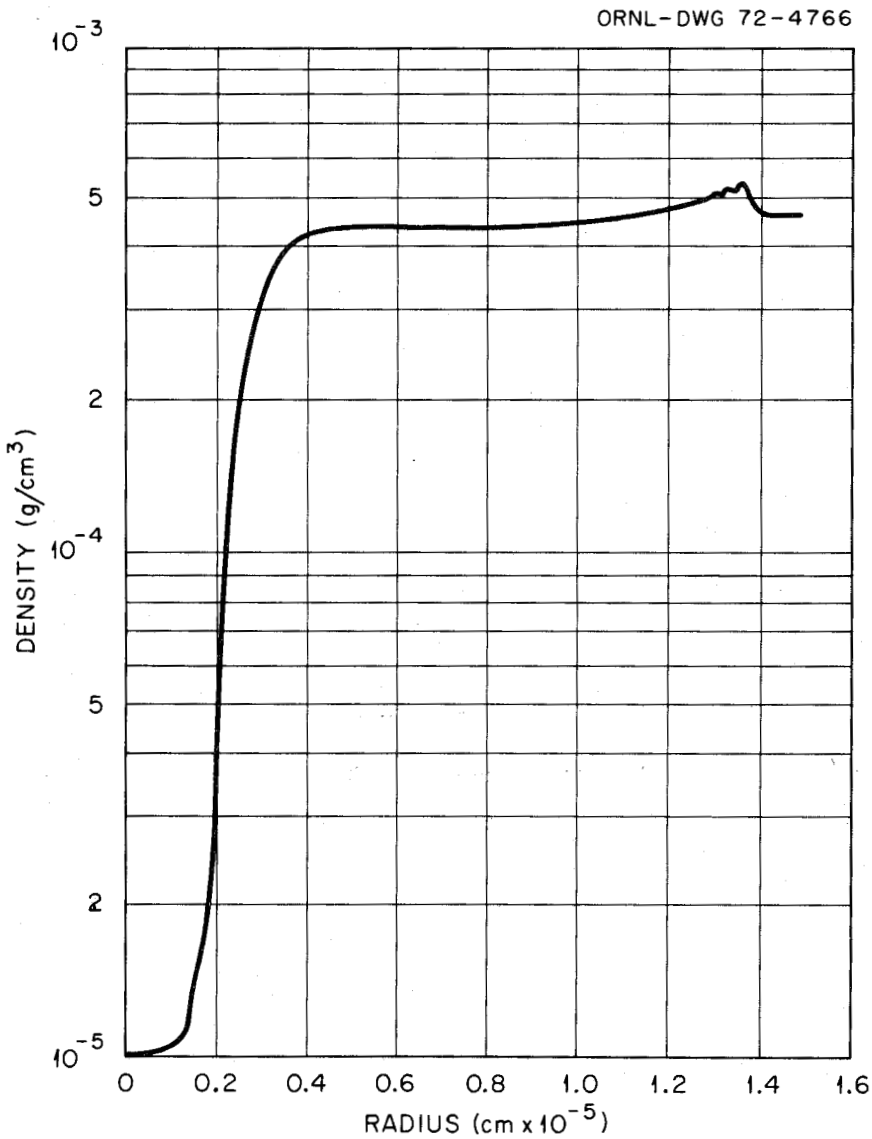

Fig. 1. Air Density Profile Around First Detonation at T = 3.16 sec.

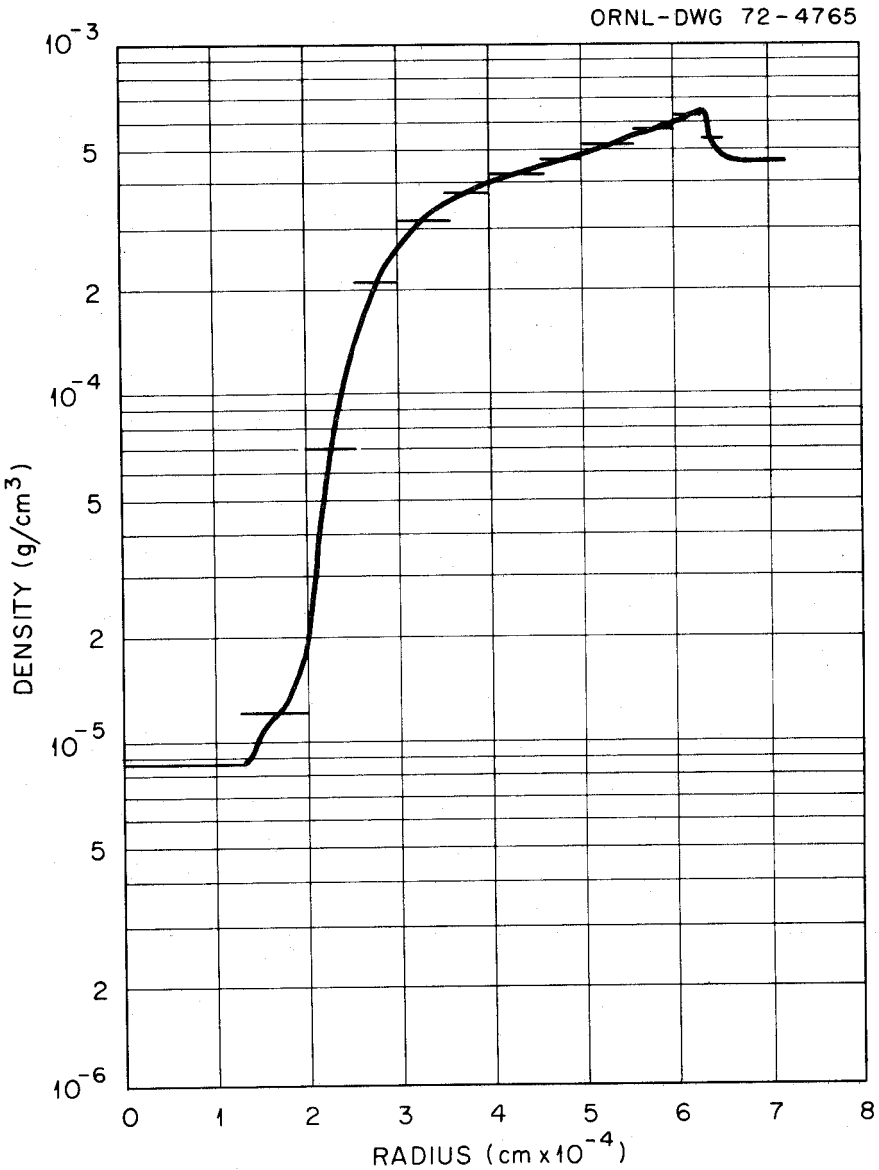

Fig. 2. Air Density Profile Around First Detonation at T = 1 sec.

Table 1. Energy Spectrum of Thermonuclear Source

Energy Group	Upper Neutron Energy (eV)	Fraction of Emission Spectrum
1	1.50(+7)[a]	0.0706
2	1.22(+7)	0.0256
3	1.00(+7)	0.0141
4	8.18(+6)	0.0147
5	6.36(+6)	0.0180
6	4.96(+6)	0.0170
7	4.06(+6)	0.0260
8	3.01(+6)	0.0190
9	2.46(+6)	0.0050
10	2.35(+6)	0.0280
11	1.83(+6)	0.0620
12	1.11(+6)	0.0850
13	5.50(+5)	0.1020
14	1.11(+5)	0.3650
15	3.35(+3)	0.1220
16	5.83(+2)	0.0240
17	1.01(+2)	0.0020
18	2.90(+1)	0

[a]Read: 1.50×10^7 eV = 15 MeV.

shown in Table 3. The angular bins are defined by a range of values of the cosine of the angle from the axis passing through the centers of both bursts. The end of the first angular bin in Problems 1, 2, 3A, 3B, and 3C approximates the tangent to the nearly void volume surrounding the first burst.

Most of the calculations were performed with the MORSE Monte Carlo code,[2] with check calculations made with the ANISN discrete ordinates code[3] in both forward and adjoint modes. The cross sections for nitrogen and oxygen, in 22 neutron groups and 18 gamma-ray groups, were from a 1970 ENDF/B-II evaluation by P. G. Young and D. G. Foster, Jr., of Los Alamos Scientific Laboratory. The neutron displacement response functions corresponding to the 22 neutron groups are given in Table 4, and the gamma-ray response functions corresponding to the 18 gamma-ray groups are shown in Table 5 (ref. 4).

In order to expedite the MORSE calculations, the code's spherical geometry routine was used with a collision density estimator of the contributions to the various responses. This method, which was also used in a recent study of the effects of the asymmetric emission of radiation from a weapon,[5] has the obvious shortcoming of too few collisions in the near-void region close to the first burst to allow an accurate determination in this region. At least three techniques exist which are superior to this method. They can be summarized as follows:

(1) Using the code's general-geometry routine so that two sets of spherical surfaces could be specified, one set around each burst. The surfaces around the first burst would define the density profiles and those around the second burst would be the surfaces used by the boundary crossing estimator routine. Dummy material numbers would be needed for each region created by the intersection of the two systems and a special GTMED routine would be necessary to distinguish between materials which are really different.

(2) Using the density estimator with pseudo collisions in the near-void volume.

Table 2. Description of Problems

Problem	Density Profile	Second Source	Distance Between Sources (m)	Fig. No.
1	At 3.16 sec	Standard thermonuclear	1500	3
2	At 3.16 sec	Standard thermonuclear	1100	4
3A	At 1 sec	Standard thermonuclear	800	5
3B	At 1 sec	14 MeV	800	5
3C	At 1 sec	Fission	800	5
3D	At 1 sec	14 MeV	600	6
3E	At 1 sec	14 MeV	300	7
3F	At 1 sec	14 MeV	0	8

ORNL-DWG 72-4671

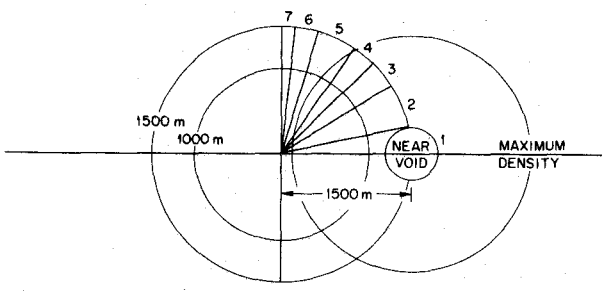

Fig. 3. Geometry for Problem 1.

ORNL-DWG 72-4672

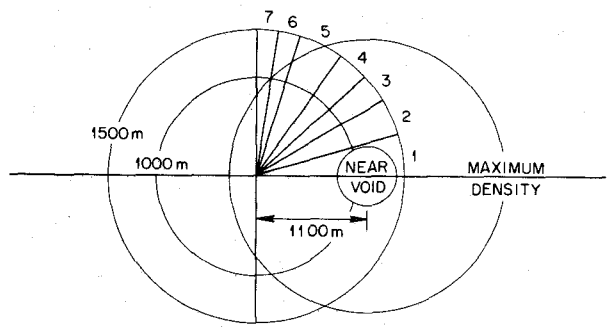

Fig. 4. Geometry for Problem 2.

ORNL-DWG 72-4673

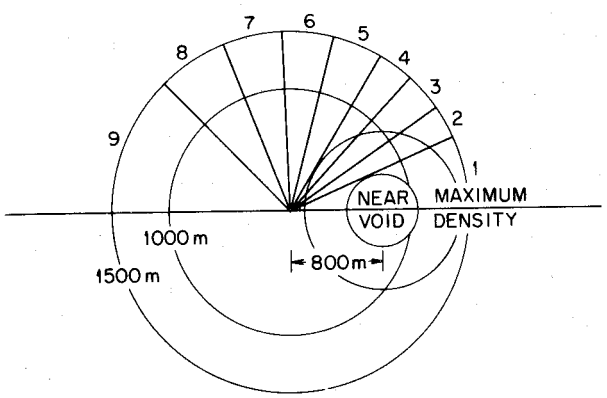

Fig. 5. Geometry for Problems 3A, 3B, and 3C.

ORNL-DWG 72-4674

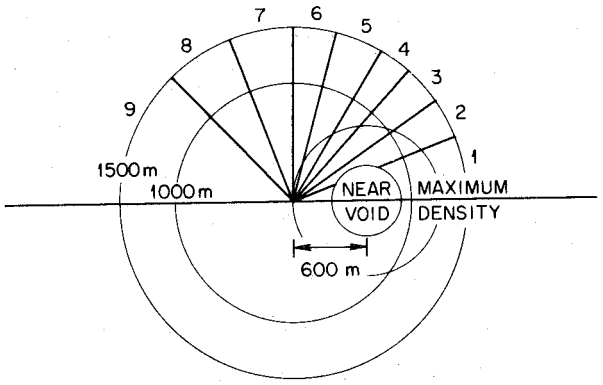

Fig. 6. Geometry for Problem 3D.

ORNL-DWG 72-4675

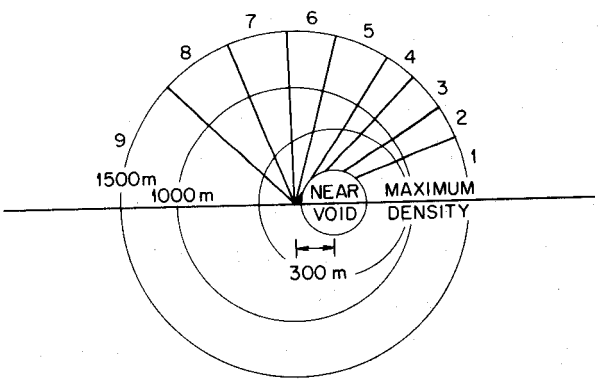

Fig. 7. Geometry for Problem 3E.

ORNL-DWG 72-4676

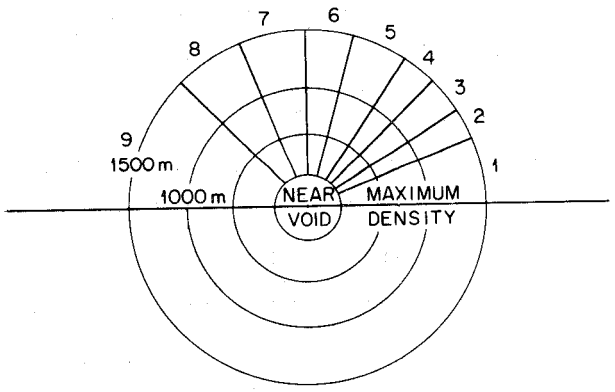

Fig. 8. Geometry for Problem 3F.

(3) Using MORSE in the adjoint mode with the response as the source where the statistics are inadequate, and using a last-flight collision estimator to calculate back to the original source point.

After all the problems listed in Table 2 were calculated with MORSE for the spherical geometry with a collision density estimator, some additional MORSE calculations were performed by the second technique listed above. In these calculations the cross sections in the near-void region were increased to their unperturbed value to ensure a more accurate collision-density estimation. The collision routine was altered to test whether a collision was a real collision or a pseudo collision, depending on the actual density. If it was determined that a pseudo collision had occurred, the particle was allowed to continue with its previous energy and direction (that is, as if no collision had occurred). If a real collision was sampled it was treated as usual.

Except for a special calculation discussed near the end of this paper, all the results presented here are for radial distances of 1000 m and 1500 m from the second burst. The relationship of these radial distances to the near-void region of the first burst in the various angular bins is shown in Figs. 3 through 8.

III. Displacement and Ionization Responses for Unperturbed Atmosphere

The neutron and secondary gamma-ray responses calculated for the case of an unperturbed atmosphere for each of the three "second-burst" sources are given in Table 6. All errors quoted on the MORSE results are 1 standard deviation. Results from the ANISN check calculations are included in the table for the 1500-m distance. These comparisons show that the MORSE estimation routines were correct at least for the neutron responses. The low MORSE results for the gamma-ray responses from the fission and thermonuclear sources indicate that the statistics are not good enough and probably that the assumed time cutoff of 1 sec was too short. However, in the calculations for the perturbed atmosphere, the density profile would also be changing with time so that using a longer time cutoff would not be realistic.

Table 3. Description of Radial Bins

Radial Bin No.	Distance from Second Source (m)	Distance Corresponding to Bin Midpoint (m)
1	750-950	850
2	950-1050	1000
3	1050-1150	1100
4	1150-1250	1200
5	1250-1350	1300
6	1350-1450	1400
7	1450-1550	1500
8	1550-1750	1650

Table 4. Neutron Energy Group Structure and Displacement Response Functions

Energy Group	Upper Neutron Energy (eV)	Response Function $\left[\frac{\text{(equiv. 1-MeV neutrons/cm}^2)}{\text{(neutron/cm}^2)}\right]$
1	1.50(+7)[a]	2.51
2	1.22(+7)	2.40
3	1.00(+7)	2.48
4	8.18(+6)	2.21
5	6.36(+6)	1.99
6	4.96(+6)	1.86
7	4.06(+6)	1.75
8	3.01(+6)	1.72
9	2.46(+6)	1.64
10	2.35(+6)	1.49
11	1.83(+6)	1.22
12	1.11(+6)	0.87[b]
13	5.50(+5)	0.59
14	1.11(+5)	0.02
15-22	<3.35(+3)	0
		22.75

[a]Read: 1.50×10^7 eV (= 15 MeV).

[b]This response function should have been 0.97.

Table 5. Gamma-Ray Energy Group Structure and Ionization Response Functions

Energy Group	Upper Gamma-Ray Energy (MeV)	Response Function $\left[\frac{\text{(rads-Si)}}{\text{(photon/cm}^2\text{)}}\right]$
1	10.0	2.83(-9)[a]
2	8.0	2.28(-9)
3	6.5	1.83(-9)
4	5.0	1.46(-9)
5	4.0	1.17(-9)
6	3.0	9.62(-10)
7	2.5	8.15(-10)
8	2.0	6.90(-10)
9	1.66	5.89(-10)
10	1.33	4.84(-10)
11	1.0	3.93(-10)
12	0.8	3.19(-10)
13	0.6	2.35(-10)
14	0.4	1.68(-10)
15	0.3	1.17(-10)
16	0.2	7.60(-11)
17	0.1	1.02(-10)
18	0.05	9.57(-10)
		1.548(-8)

[a]Read: 2.83×10^{-9}.

Table 6. Neutron and Gamma-Ray Responses in an Unperturbed Atmosphere at 1000 m and 1500 m from Various Sources

Source	Neutron Displacement $\left[\frac{\text{Equiv. 1-MeV neutrons/cm}^2}{\text{source neutron}}\right]$		Gamma-Ray Ionization $\left[\frac{\text{rads-Si}}{\text{source neutron}}\right]$	
	1000 m	1500 m	1000 m	1500 m
		MORSE Calculations[a]		
Thermonuclear	$(5.50 \pm 0.10) \times 10^{-12}$	$(1.36 \pm 0.04) \times 10^{-12}$	$(1.05 \pm 0.09) \times 10^{-21}$	$(3.0 \pm 0.3) \times 10^{-22}$
14-MeV[b]	$(1.61 \pm 0.05) \times 10^{-11}$	$(4.43 \pm 0.12) \times 10^{-12}$	$(5.14 \pm 0.10) \times 10^{-21}$	$(1.75 \pm 0.05) \times 10^{-21}$
Fission[b]	$(1.09 \pm 0.03) \times 10^{-11}$	$(2.66 \pm 0.11) \times 10^{-12}$	$(4.3 \pm 2) \times 10^{-22}$	$(1.2 \pm 0.2) \times 10^{-22}$
		ANISN Forward Calculations		
Thermonuclear	-	1.38×10^{-12}	-	4.03×10^{-22}
14-MeV	-	4.44×10^{-12}	-	1.77×10^{-21}
Fission	-	2.67×10^{-12}	-	2.17×10^{-22}
		ANISN Adjoint Calculations		
Thermonuclear	-	1.38×10^{-12}	-	4.02×10^{-22}
14-MeV	-	4.45×10^{-12}	-	1.77×10^{-21}
Fission	-	2.68×10^{-12}	-	2.16×10^{-22}

[a]Quoted errors are 1 standard deviation.

[b]These unperturbed results are averages of the results obtained for the three backward angles (7-9) in Problems 3B and 3C for the 14-MeV and fission source respectively.

The real and adjoint ANISN calculations are in good agreement for all sources.

IV. Displacement and Ionization Responses for Perturbed Atmosphere

Problem 1

Problem 1 is for the case of the 3.16-sec density profile (Fig. 1) and the thermonuclear source detonated at a distance of 1500 m from the first burst (see Fig. 3). The ratios of the neutron and gamma-ray responses in the perturbed atmosphere to those in the unperturbed atmosphere are given in Table 7.

An examination of the response ratios shows that they do not deviate from unity significantly, indicating that in this case the perturbation created by the first burst had little effect. The point at 1500 m in the first angular bin is in the near-void volume, but even so the neutron response is increased by only 20%, which is less than half a standard deviation. The near-void volume subtends only a small angle at the thermonuclear source position; the solid angle subtended by the first angular bin, which approximates the tangent to the void, is only 1/14th of that of the other angular bins. This small angle, plus the lack of collisions within the void, complicates the calculation. The 13% rise in the neutron response in the second angular bin at 1500 m is only slightly different from unity. The statistics on the gamma-ray responses are not good enough for any conclusions to be drawn about them.

An additional MORSE calculation for Problem 1 in which pseudo collisions were allowed in the near-void region yielded a neutron response ratio of 1.02 ± 0.28 for the first angular bin at 1500 m. This is an improvement over the calculation with the collision density estimator, but still is not accurate. A better ratio was obtained by running adjoint ANISN calculations for both the perturbed and the unperturbed atmospheres with the neutron response used as the source at the origin of the spherical geometry (that is, at the point of the first detonation). A calculation of this type shows the importance of the second source at a distance R in causing a response at the point of the first detonation. The results of

Table 7. Ratio of Detector Responses in Perturbed Air to Responses in Unperturbed Air for Problems 1 and 2[a] (MORSE Calculations)

Angular Bin	Cosθ	θ	Ratio: Perturbed Response/Unperturbed Response			
			Neutrons		Gamma Rays	
			R = 1000 m	R = 1500 m	R = 1000 m	R = 1500 m
Prob. 1: 3.16-sec Profile; Thermonuclear Source at 1500 m						
1	1.0-0.99	0-8	0.77 ± 0.11	1.20 ± 0.45	1.41 ± 0.52	-
2	0.99-0.86	8-31	0.94 ± 0.05	1.13 ± 0.06	0.95 ± 0.15	1.20 ± 0.11
3	0.86-0.71	31-45	0.95 ± 0.05	0.99 ± 0.05	1.15 ± 0.16	1.57 ± 0.19
4	0.71-0.57	45-57	0.95 ± 0.05	0.88 ± 0.05	3.0 ± 2.1	1.10 ± 0.11
5	0.57-0.29	57-73	0.93 ± 0.04	0.98 ± 0.05	0.88 ± 0.06	1.47 ± 0.3
6	0.29-0.14	73-82	0.98 ± 0.05	0.94 ± 0.07	1.00 ± 0.15	1.10 ± 0.16
7	0.14-0	82-90	0.89 ± 0.05	0.98 ± 0.08	0.92 ± 0.13	0.96 ± 0.08
Prob. 2: 3.16-sec Profile; Thermonuclear Source at 1100 m						
1	1.0-0.98	0-12	0.95 ± 0.30	1.57 ± 0.10	1.0 ± 0.9	2.3 ± 0.8
2	0.98-0.86	12-31	0.97 ± 0.05	1.18 ± 0.05	1.24 ± 0.17	1.01 ± 0.07
3	0.86-0.71	31-45	1.08 ± 0.04	1.07 ± 0.05	0.90 ± 0.09	1.24 ± 0.06
4	0.71-0.57	45-57	1.07 ± 0.04	1.13 ± 0.05	1.40 ± 0.25	1.5 ± 0.5
5	0.57-0.29	57-73	1.06 ± 0.03	1.04 ± 0.05	1.05 ± 0.10	0.98 ± 0.07
6	0.29-0.14	73-82	1.01 ± 0.04	1.09 ± 0.08	0.84 ± 0.07	1.5 ± 0.2
7	0.14-0	82-90	0.92 ± 0.07	0.92 ± 0.07	0.81 ± 0.08	1.04 ± 0.13

[a]Unperturbed responses given in Table 6.

the ANISN calculations are compared with those from the MORSE calculations in Table 8. The ratios of 1.16 for neutrons and 1.08 for gamma rays should be the maximum variations at 1500 m.

Problem 2

Problem 2 is for the case of the 3.16-sec profile (Fig. 1) and the thermonuclear source detonated 1100 m from the first burst (see Fig. 4). The ratios of the neutron and gamma-ray responses in the perturbed atmosphere to those in the unperturbed atmosphere are included in Table 7.

In this case the ratio of the neutron responses for the first angular bin at 1500 m shows a significant deviation from unity (ratio = 1.57 $\pm$ 0.10). This position is just beyond the near-void volume and should be the position at which the maximum possible variation occurs. The second angular bin at 1500 m also shows a slightly significant deviation from unity. As was the case for Problem 1, the statistics on the gamma-ray results are poor. For both Problems 1 and 2, path length stretching was employed in the MORSE calculations to increase the number of neutrons near the first detonation.

Problems 3A, 3B, and 3C

Problems 3A, 3B, and 3C are for the case of a 1-sec profile (Fig. 2) and an 800-m separation distance of the two weapons, the second source being the thermonuclear source, the 14-MeV source, and the fission source respectively. The geometry for all three problems is shown in Fig. 5, and the corresponding neutron and gamma-ray response ratios are given in Table 9. For these calculations path-length stretching was employed in the MORSE calculations to remove neutrons from the vicinity of the second source.

In all three problems, the neutron response ratios for the first angular bin show that the neutron response is considerably higher in the perturbed atmosphere than in the unperturbed atmosphere. A significant deviation from unity is observed in the first angular bin for the gamma-ray response for the 14-MeV source.

Table 8. Comparison of Problem 1 Detector Response Ratios Obtained by Different Methods for Angular Bin 1 at R = 1500 m

Calculational Method	Ratio: Perturbed Response/Unperturbed Response	
	Neutrons	Gamma Rays
MORSE	1.20 ± 0.45	
MORSE with pseudo collisions in near-void volume	1.02 ± 0.28	
ANISN adjoint	1.16	1.08

Problems 3D, 3E, and 3F

Problems 3D, 3E, and 3F are for the case of the 1-sec profile (Fig. 2) and the 14-MeV source at distances of 600, 300, and 0 m respectively from the first detonation. The geometries for these problems are shown in Figs. 6, 7, and 8, and the corresponding response ratios are given in Table 10. Again path-length stretching was employed in the MORSE calculations to remove neutrons from the vicinity of the source. In all these cases for the 14-MeV source the statistics on the gamma-ray responses are considered to be good enough for comparisons between responses in the perturbed and unperturbed atmospheres to be significant.

In Problem 3D significant increases in the responses in the perturbed atmosphere are apparent for the first two bins at both distances for both neutrons and gamma rays, the increase for neutrons in the first angular bin at the 1000-m distance being the largest observed in this study. Significant deviations from unity occur in the first five angular bins for both the neutron and gamma-ray responses in Problem 3E, and in all angular bins in Problem 3F.

In Problem 3F, in which case the two bursts are at the same point, the neutron response in the perturbed atmosphere increases over the response in the unperturbed atmosphere in all angular bins by about 20% at both the 1000-m range and the 1500-m range. The corresponding increase in gamma-ray responses is about 10%.

These calculations for the coincident burst points were verified by ANISN calculations in the forward mode.

V. Neutron and Gamma-Ray Fluxes Produced by 14-MeV Neutron Source

Tables 11 and 12 respectively show the neutron and gamma-ray fluxes obtained from ANISN calculations for a position 1000 m from the 14-MeV source located at the position of the first burst. The fluxes are given for each energy group for both unperturbed and perturbed atmospheres, the latter described by the 1-sec and the 3.16-sec density profiles. By applying the appropriate response function any required response can be calculated from these fluxes.

Table 9. Ratio of Detector Responses in Perturbed Air to Responses in Unperturbed Air for Problems 3A, 3B, and 3C[a] (MORSE Calculations)

Angular Bin	Cosθ	θ	Ratio: Perturbed Response/Unperturbed Response — Neutrons R = 1000 m	Neutrons R = 1500 m	Gamma Rays R = 1000 m	Gamma Rays R = 1500 m
			Prob. 3A: 1-sec Profile; Thermonuclear Source at 800 m			
1	1.0 - 0.955	0-17	1.51 ± 0.42	1.57 ± 0.26	0.78 ± 0.25	0.98 ± 0.13
2	0.955 - 0.86	17-31	1.09 ± 0.08	0.96 ± 0.10	0.73 ± 0.12	1.08 ± 0.14
3	0.86 - 0.71	31-45	0.96 ± 0.08	0.99 ± 0.09	0.88 ± 0.12	0.87 ± 0.14
4	0.71 - 0.57	45-57	0.88 ± 0.07	0.85 ± 0.06	0.87 ± 0.11	1.05 ± 0.13
5	0.57 - 0.29	57-73	1.00 ± 0.05	1.05 ± 0.09	0.88 ± 0.11	0.92 ± 0.10
6	0.29 - 0	73-90	1.17 ± 0.05	1.08 ± 0.07	0.89 ± 0.10	1.95 ± 0.76
7	0 - -0.33	90-109	1.04 ± 0.05	0.97 ± 0.06	0.76 ± 0.08	0.97 ± 0.07
8	-0.33 - -0.67	109-132	0.93 ± 0.04	1.02 ± 0.06	0.96 ± 0.11	1.17 ± 0.22
9	-0.67 - -1.0	132-180	1.11 ± 0.08	1.10 ± 0.09	1.04 ± 0.10	0.84 ± 0.08
			Prob. 3B: 1-sec Profile; 14-MeV Source at 800 m			
1	1.0 - 0.955	0-17	1.52 ± 0.24	1.50 ± 0.12	1.33 ± 0.22	1.42 ± 0.13
2	0.955 - 0.86	17-31	1.04 ± 0.06	1.14 ± 0.08	1.05 ± 0.07	0.96 ± 0.07
3	0.86 - 0.71	31-45	1.00 ± 0.06	0.97 ± 0.06	1.05 ± 0.06	0.89 ± 0.06
4	0.71 - 0.57	45-57	0.89 ± 0.05	1.06 ± 0.06	0.92 ± 0.06	1.06 ± 0.07
5	0.57 - 0.29	57-73	0.91 ± 0.04	0.97 ± 0.05	1.04 ± 0.05	0.99 ± 0.04
6	0.29 - 0	73-90	1.00 ± 0.04	1.01 ± 0.04	1.02 ± 0.04	0.97 ± 0.04
7	0 - -0.33	90-109	0.97 ± 0.04	1.91 ± 0.04	1.01 ± 0.04	0.97 ± 0.06
8	-0.33 - -0.67	109-132	0.99 ± 0.04	0.94 ± 0.04	1.01 ± 0.03	0.97 ± 0.04
9	-0.67 - -1.0	132-180	1.05 ± 0.04	1.05 ± 0.05	0.98 ± 0.04	1.06 ± 0.04
			Prob. 3C: 1-sec Profile; Fission Source at 800 m			
1	1.0 - 0.955	0-17	1.62 ± 0.19	1.37 ± 0.18	2.9 ± 1.2	1.08 ± 0.30
2	0.955 - 0.86	17-31	1.24 ± 0.08	1.02 ± 0.08	0.94 ± 0.27	2.1 ± 0.8
3	0.86 - 0.71	31-45	0.89 ± 0.06	1.15 ± 0.08	1.03 ± 0.35	1.43 ± 0.58
4	0.71 - 0.57	45-57	0.99 ± 0.08	0.89 ± 0.07	0.67 ± 0.18	1.48 ± 0.50
5	0.57 - 0.29	57-73	0.06 ± 0.05	1.08 ± 0.06	0.86 ± 0.20	0.79 ± 0.18
6	0.29 - 0	73-90	1.00 ± 0.04	1.07 ± 0.08	0.52 ± 0.16	0.95 ± 0.34
7	0 - -0.33	90-109	1.06 ± 0.04	1.06 ± 0.06	0.50 ± 0.20	0.85 ± 0.16
8	-0.33 - -0.67	109-132	0.94 ± 0.04	0.95 ± 0.04	2.8 ± 2.1	1.19 ± 0.30
9	-0.67 - -1.0	132-180	0.99 ± 0.04	1.00 ± 0.07	0.64 ± 0.20	0.95 ± 0.16

[a]Unperturbed responses given in Table 6.

Table 10. Ratio of Detector Responses in Perturbed Air to Responses in Unperturbed Air for Problems 3D, 3E, and 3F[a,b] (MORSE Calculations)

Angular Bin	Cosθ	θ	Ratio: Perturbed Response/Unperturbed Response — Neutrons R = 1000 m	Neutrons R = 1500 m	Gamma Rays R = 1000 m	Gamma Rays R = 1500 m
			Prob. 3D: 1-sec Profile; 14-MeV Source at 600 m			
1	1.0 - 0.93	0-22	1.93 ± 0.16	1.58 ± 0.11	1.48 ± 0.10	1.54 ± 0.14
2	0.93 - 0.86	22-31	1.24 ± 0.08	1.10 ± 0.07	1.23 ± 0.08	1.19 ± 0.10
3	0.86 - 0.71	31-45	0.98 ± 0.06	1.05 ± 0.06	1.04 ± 0.05	0.97 ± 0.06
4	0.71 - 0.57	45-57	0.89 ± 0.05	0.98 ± 0.06	0.98 ± 0.05	1.00 ± 0.09
5	0.57 - 0.29	57-73	0.90 ± 0.04	0.93 ± 0.04	0.99 ± 0.04	1.11 ± 0.18
6	0.29 - 0	73-90	0.89 ± 0.03	0.91 ± 0.04	0.94 ± 0.04	0.99 ± 0.05
7	0 - -0.33	90-109	0.98 ± 0.03	0.93 ± 0.04	1.01 ± 0.04	0.94 ± 0.04
8	-0.33 - -0.67	109-132	1.06 ± 0.04	1.03 ± 0.04	1.04 ± 0.04	1.10 ± 0.05
9	-0.67 - -1.0	132-180	1.00 ± 0.04	1.09 ± 0.07	1.02 ± 0.04	0.94 ± 0.04
			Prob. 3E: 1-sec Profile; 14-MeV Source at 300 m			
1	1.0 - 0.93	0-22	1.68 ± 0.10	1.60 ± 0.12	1.44 ± 0.11	1.46 ± 0.11
2	0.93 - 0.86	22-31	1.48 ± 0.08	1.31 ± 0.09	1.46 ± 0.11	1.27 ± 0.10
3	0.86 - 0.71	31-45	1.43 ± 0.07	1.45 ± 0.09	1.29 ± 0.07	1.20 ± 0.06
4	0.71 - 0.57	45-57	1.34 ± 0.07	1.30 ± 0.09	1.05 ± 0.05	1.03 ± 0.04
5	0.57 - 0.29	57-73	0.90 ± 0.04	0.93 ± 0.04	0.99 ± 0.04	1.11 ± 0.18
6	0.29 - 0	73-90	0.99 ± 0.04	1.08 ± 0.05	1.07 ± 0.05	1.03 ± 0.05
7	0 - -0.33	90-109	0.98 ± 0.04	1.02 ± 0.04	1.05 ± 0.04	1.06 ± 0.04
8	-0.33 - -0.67	109-132	0.97 ± 0.04	1.02 ± 0.05	0.96 ± 0.04	0.95 ± 0.04
9	-0.67 - -1.0	132-180	0.94 ± 0.03	0.92 ± 0.04	0.99 ± 0.04	0.86 ± 0.04
			Prob. 3F: 1-sec Profile; 14-MeV Source at 0 m			
1	1.0 - 0.93	0-22	1.04 ± 0.08	1.15 ± 0.09	1.14 ± 0.09	1.21 ± 0.10
2	0.93 - 0.86	22-31	1.18 ± 0.09	1.10 ± 0.09	1.21 ± 0.12	1.04 ± 0.08
3	0.86 - 0.71	31-45	1.24 ± 0.06	1.26 ± 0.06	1.03 ± 0.06	1.15 ± 0.06
4	0.71 - 0.57	45-57	1.14 ± 0.05	1.16 ± 0.06	1.03 ± 0.06	1.12 ± 0.08
5	0.57 - 0.29	57-73	1.19 ± 0.04	1.17 ± 0.05	1.01 ± 0.05	1.10 ± 0.04
6	0.29 - 0	73-90	1.22 ± 0.04	1.13 ± 0.04	1.07 ± 0.04	1.07 ± 0.04
7	0 - -0.33	90-109	1.14 ± 0.04	1.23 ± 0.04	1.06 ± 0.04	1.13 ± 0.04
8	-0.33 - -0.67	109-132	1.18 ± 0.04	1.23 ± 0.04	1.11 ± 0.04	1.06 ± 0.04
9	-0.67 - -1.0	132-180	1.17 ± 0.04	1.24 ± 0.06	1.04 ± 0.04	1.01 ± 0.03
Average			1.18 ± 0.02	1.20 ± 0.02	1.07 ± 0.02	1.10 ± 0.02

[a]Unperturbed responses given in Table 6.

[b]Results for 14-MeV source at 800 m given in Table 9.

Table 11. Neutron Fluxes Produced 1000 m from 14-MeV Source for Case of Coincident Burst Points (ANISN Forward Calculations)

Group No.	Upper Neutron Energy (eV)	Neutron Flux [(neutrons $cm^{-2} \cdot sec^{-1}$)/(source neutron/sec)]		
		Unperturbed Air	1-sec Profile	3.16-sec Profile
1	1.50(+7)[a]	14.72(-13)	23.11(-13)	23.95(-13)
2	1.22(+7)	7.59(-13)	9.10(-13)	9.44(-13)
3	1.00(+7)	3.73(-13)	4.02(-13)	4.15(-13)
4	8.18(+6)	3.89(-13)	4.24(-13)	4.37(-13)
5	6.36(+6)	5.22(-13)	5.72(-13)	5.89(-13)
6	4.96(+6)	4.40(-13)	4.75(-13)	4.90(-13)
7	4.06(+6)	4.97(-13)	5.43(-13)	5.62(-13)
8	3.01(+6)	4.61(-13)	4.92(-13)	5.08(-13)
9	2.46(+6)	1.36(-13)	1.41(-13)	1.46(-13)
10	2.35(+6)	6.29(-13)	6.49(-13)	6.69(-13)
11	1.83(+6)	11.19(-13)	11.29(-13)	11.60(-13)
12	1.11(+6)	15.69(-13)	15.37(-13)	15.72(-13)
13	5.50(+5)	22.13(-13)	21.36(-13)	21.81(-13)
14	1.11(+5)	28.55(-13)	26.91(-13)	27.35(-13)
15	3.35(+3)	10.75(-13)	10.05(-13)	10.19(-13)
16	5.83(+2)	9.55(-13)	8.86(-13)	8.97(-13)
17	1.01(+2)	6.27(-13)	5.79(-13)	5.86(-13)
18	2.90(+1)	4.71(-13)	4.34(-13)	4.39(-13)
19	1.07(+1)	5.35(-13)	4.91(-13)	4.96(-13)
20	3.06(+0)	3.70(-13)	3.38(-13)	3.41(-13)
21	1.12(+0)	2.99(-13)	2.73(-13)	2.75(-13)
22	4.14(-1)	2.37(-13)	2.16(-13)	2.18(-13)

[a]Read: 1.50×10^7.

Table 12. Gamma-Ray Fluxes Produced 1000 m from 14-MeV Source for Case of Coincident Burst Points (ANISN Forward Calculations)

Group No.	Upper Gamma-Ray Energy (eV)	Gamma-Ray Fluxes [(Photons $cm^{-2} \cdot sec^{-1}$)/(source neutron/sec)]		
		Unperturbed Air	1-sec Profile	3-sec Profile)
1	10.0	0.34(-13)[a]	0.37(-13)	0.37(-13)
2	8.0	4.51(-13)	4.98(-13)	5.10(-13)
3	6.5	6.39(-13)	6.89(-13)	7.04(-13)
4	5.0	3.77(-13)	4.09(-13)	4.18(-13)
5	4.0	4.46(-13)	4.87(-13)	4.98(-13)
6	3.0	1.57(-13)	1.64(-13)	1.67(-13)
7	2.5	4.90(-13)	5.29(-13)	5.42(-13)
8	2.0	1.38(-13)	1.36(-13)	1.36(-13)
9	1.66	2.68(-13)	2.79(-13)	2.84(-13)
10	1.33	2.21(-13)	2.21(-13)	2.23(-13)
11	1.0	1.63(-13)	1.60(-13)	1.61(-13)
12	0.8	2.67(-13)	2.74(-13)	2.78(-13)
13	0.6	6.05(-13)	6.13(-13)	6.24(-13)
14	0.4	4.11(-13)	4.08(-13)	4.16(-13)
15	0.3	7.56(-13)	7.53(-13)	7.66(-13)
16	0.2	22.3(-13)	21.6(-13)	22.0(-13)
17	0.1	29.6(-13)	28.0(-13)	28.4(-13)
18	0.05	1.28(-13)	1.21(-13)	1.23(-13)

[a]Read: 0.34×10^{-13}.

VI. Importance of 14-MeV Neutrons Born at Radius R to Responses at Origin of Spherical Geometry

Table 13 presents the results from adjoint ANISN calculations in which the source was assumed to consist of 14-MeV neutrons born at radius R in a spherical geometry and the position of the response was taken at the origin. From these calculations the importance of 14-MeV neutrons born at radius R to the response at the origin can be determined. The responses calculated were neutron displacement and gamma-ray ionization for both unperturbed and perturbed atmospheres, the latter described by the 1-sec and the 3.16-sec density profiles.

The neutron response ratios show a slight maximum at a radius of about 500 m for the 1-sec profile and at about 1200 m for the 3.16-sec profile. These radii are slightly less than the corresponding radii for the maximum air density. Beyond these values the ratios are constant. The ratios of the gamma-ray responses are at first less than unity and then increase to greater than unity as the distance from the source increases.

VII. Summary

In general, the effects of the density perturbations for Problems 1 and 2 are small. This was expected since the perturbations reflected in the 3.16-sec density profile itself are small except for a small void at the detonation center which did not subtend a large solid angle at the second source. For Problems 3A through 3F, the effects are greater for all sources. This, too, was expected since the 1-sec density profile has much larger perturbations and the second source is closer to the first source in all cases; thus, the void formed at the center of the first source subtends a larger solid angle at the second source. All neutron responses calculated for positions immediately beyond the first burst are about 50% higher than those obtained at the same positions in the unperturbed atmosphere; lesser increases were obtained as the angle from the axis of symmetry was increased. The secondary gamma-ray responses also are higher, with the increases being approximately one-half of the increases of the neutron responses at the same positions. For the case of the two detonations occurring at the same position (Problem 3F), the

Table 13. Importance of 14-MeV Neutrons Born at Radius R to Response at Origin of Spherical Geometry: Ratio of Responses in Perturbed Air to Responses in Unperturbed Air (ANISN Adjoint Calculations)

Radius R (m)	Neutrons			Gamma Rays		
	Unperturbed Response[a]	Ratio: Perturbed Response/Unperturbed Response		Unperturbed Response[b]	Ratio: Perturbed Response/Unperturbed Response	
		1-sec Profile	3.16-sec Profile		1-sec Profile	3.16-sec Profile
13.5	1.17E-7	1.00	1.00	1.66-18	0.032	0.038
10.5	1.92E-9	0.96	0.96	1.77-19	0.15	0.17
205	5.22-10	1.01	1.03	7.74-20	0.33	0.39
305	2.40-10	1.14	1.15	4.52-20	0.59	0.67
405	1.35-10	1.22	1.17	2.97-20	0.78	0.80
505	8.50-11	1.25	1.18	2.08-20	0.90	0.88
605	5.70-11	1.23	1.19	1.51-20	0.96	0.93
760	3.33-11	1.19	1.20	9.76-21	0.98	0.99
960	1.82-11	1.18	1.22	5.87-21	1.03	1.05
1160	1.05-11	1.18	1.23	3.68-21	1.07	1.10
1360	6.34-12	1.18	1.21	2.38-21	1.09	1.10
1560	3.91-12	1.18	1.20	1.57-21	1.11	1.11
2172	9.39-13	1.18	1.19	4.59-22	1.15	1.15

[a] In neutron displacement units [(equiv. 1-MeV neutrons/cm^2)/ (source neutron)].

[b] In gamma-ray ionization units [(rads-Si)/ (source neutron)].

neutron responses between 1000 and 1500 m are about 20% higher than those in the unperturbed atmosphere and the gamma-ray responses are 10% higher.

These MORSE calculations could easily be extended to investigate the effects of density changes on the time-dependent response rates.

References

1. Supplied to C. E. Clifford, Oak Ridge National Laboratory, by B. C. Diven, Los Alamos Scientific Laboratory, 1967.

2. E. A. Straker, P. N. Stevens, D. C. Irving, and V. R. Cain, "The MORSE Code - A Multigroup Neutron and Gamma-Ray Monte Carlo Transport Code," ORNL-4585 (1970).

3. W. W. Engle, Jr., "A User's Manual for ANISN, A One-Dimensional Discrete Ordinates Transport Code with Anisotropic Scattering," informal notes included in RSIC Computer Code Collection CCC-89, Oak Ridge National Laboratory.

4. E. A. Straker and M. L. Gritzner, "Neutron and Secondary Gamma-Ray Transport in Infinite Homogeneous Air," ORNL-4464 (1969).

5. B. J. McGregor and E. A. Straker, "A Study of the Effect of Source Asymmetry on Time-Dependent Neutron and Secondary Gamma-Ray Transport in Air," ORNL-4741 (1972).

Internal Distribution

1-3. L. S. Abbott
4. R. G. Alsmiller
5. D. E. Bartine
6-10. C. E. Clifford
11. S. N. Cramer
12. M. B. Emmett
13. W. W. Engle, Jr.
14. M. L. Gritzner
15. N. M. Greene
16. T. J. Hoffman
17. W. H. Jordan
18. F. C. Maienschein
19-23. B. J. McGregor
24. F. R. Mynatt
25. E. M. Oblow
26. J. V. Pace, III
27. R. W. Peelle
28. F. G. Perey
29. R. W. Roussin
30. D. Sundberg
31. D. K. Trubey
32. G. E. Whitesides
33. H. Feshbach (consultant)
34. H. Goldstein (consultant)
35. C. R. Mehl (consultant)
36. H. T. Motz (consultant)
37-38. Central Research Library
39. ORNL Y-12 Technocal Library Document Reference Section
40-41. Laboratory Records Department
42. Laboratory Records ORNL RC
43. ORNL Patent Office

External Distribution

44. P. B. Hemmig, Division of Reactor Development and Technology, U. S. Atomic Energy Commission, Washington, D. C.
45. W. H. Hannum, Division of Reactor Development and Technology, U. S. Atomic Energy Commission, Washington, D. C.
46. Kermit Laughon, AEC Site Representative
47-176. Given DNA Initial Radiation Transport Distribution
177-178. Technical Information Center (TIC)
179. Research and Technical Support Division (ORO)